DESIGN OPTIMIZATION OF CONVENTIONAL HEAT PUMPS: APPLICATION TO STEADY-STATE HEATING EFFICIENCY

by

C. K. Rice S. K. Fischer R. D. Ellison W. L. Jackson

Conservation Technology Program
Energy Division
Oak Ridge National Laboratory
Oak Ridge, Tennessee

ABSTRACT

A physically-based heat pump model was connected to an optimization program to form a computer code for use in the design of high-efficiency heat pumps. The method used allows for the simultaneous optimization of selected design variables, taking proper account of their interactions, while constraining other parameters to chosen limits or fixed values.

For optimization of the steady-state heating efficiency of conventional heat pumps, ten variables were optimized while heating capacity was fixed; the results may, however, be scaled to other capacities. Calculations were made for a range of component efficiencies and heat exchanger sizes. The results predict substantial improvement in heating performance due to both optimal system configurations and the use of improved components.

Sensitivity analyses show that there is considerable latitude for deviating from the optimum design to make use of available component sizes and for accomodating the compromises needed for good cooling performance.

INTRODUCTION

Recent advances in heat pump technology have made possible the design and manufacture of heat pumps with performance characteristics substantially superior to those available only a few years ago. However, there are further opportunities to improve the efficiency and thus the energy conservation potential of conventional air-source heat pumps. This study was undertaken to explore design techniques that will optimize steady-state heating efficiency and best exploit further advances in technology. It is part of a more extensive investigation(1) of the limits of efficiency that may reasonably be expected in both the near and long-range future.

A physically-based heat pump model,(1,2,3) connected to an optimization program, was used to calculate the maximum heating coefficient of performance (COP) that can be attained both with components that are presently available and with improved ones for a range of heat exchanger sizes. The program allows the simultaneous optimization of all the selected design variables while constraining other parameters to chosen

---

This research was sponsored by the Office of Buildings and Community Systems, U.S. Department of Energy under contract W-7405-eng-26 with the Union Carbide Corporation.

C. K. Rice, R. D. Ellison and S. K. Fischer are members of the Conservation Technology Program, Energy Division, Oak Ridge National Laboratory, Oak Ridge, TN.

W. L. Jackson is a member of the Computer Sciences Division, Oak Ridge National Laboratory, Oak Ridge, TN.

limits or constant values. With this technique, the complex interactions between design parameters are taken into account. If the constraints are properly formulated, the results are independent of the heating capacity at which the heat pump design was optimized. The above procedure is in contrast to traditional methods that may optimize a few parameters at a time.

However, the heat pump configuration selected by an optimizing procedure may not be unique for the calculated COP. "Trade-offs" between some of the design parameters are usually possible. Thus there may be no "best" design, but rather a family of configurations clustered about the calculated optimum. Plots of the sensitivity of COP to changes in these variables were developed to explore the tradeoffs and other design flexibilities.

It would be presumptuous to say that the numerical results from this analytical study should be taken as manufacturing goals. Rather, when combined with preliminary estimates of cost-effectiveness of the suggested improvements,(4) these numerical results are of interest in setting the priorities of our internal heat pump research and development program. It is, however, hoped that the design methods developed in this study will be interesting and useful to designers in the heat pump industry.

METHOD OF ANALYSIS

The basic tool used for analysis in this study is a version of our basic heat pump model previously reported by Ellison and Creswick(2) and Ellison, et al.(3) with improvements due to Rice, et al.(1) It was connected to an optimization program to calculate optimum design parameters, used alone to analyze the performance of optimized systems over a range of operating conditions, and used with another program developed for this study to find the sensitivity of COP to changes in these design parameters. A brief description of the model is included below; a more complete discussion may be found in Ref 1, 2 and 3.

General Characteristics and Assumptions in the Heat Pump Model

To the extent possible, the model is based on underlying physical principles, rather than empirical equations derived from performance data of existing heat pumps. Such a physically-based model provides more explicit detail of the interactions between the system components and is more flexible in exploring design and operating parameters that differ from present practice. This flexibility, and the details of the interactions, are necessary attributes of a model to be used in seeking optimum designs.

As used for this study, the heat pump model was organized into three principal sections: the compressor, condenser, and evaporator models. It was assumed that the refrigerant flow-control device maintains

a specified value of refrigerant subcooling at the condenser exit. It was further assumed that the heat pump being modeled contains a suction-line accumulator which remains partially filled with liquid refrigerant, and thus maintains a low value of refrigerant superheat at the compressor shell entry. This assumption is appropriate for present purposes since maximum performance is achieved with low superheat values. Both assumptions also obviate the need for sub-models of the flow control device and the inventory of refrigerant charge. Air-side pressure drops and power consumption by the fan motors are explicitly calculated. All refrigerant-side calculations were made using the properties of R-22.

Compressor Model

The compressor model is based on performance and efficiency parameters, in contrast to the use of design parameters. This approach allows some simplification while retaining sufficient detail of the underlying physical principles. The resulting model is compatible with the intended use in that predictions can be made of how changes in compressor efficiency affect the heat pump system; it cannot, however, be used to determine what specific changes in compressor design might lead to the improved efficiency.

The basic compressor model requires seven input parameters:

- compressor isentropic efficiency from suction port to discharge port
- compressor mechanical efficiency
- maximum value of the compressor motor efficiency
- shaft power of compressor motor at rated load
- synchronous motor speed
- compressor piston displacement
- effective clearance volume ratio

Using these parameters, standard motor performance curves, the suction gas conditions, and condensing pressure, the compressor model calculates:

- refrigerant state at suction port
- refrigerant mass-flow rate
- temperature of the superheated refrigerant vapor at exit from the hermetically sealed shell
- estimate of the shell heat loss
- required motor shaft power
- motor speed and efficiency
- power consumed by the motor

Initial estimates of the suction gas conditions and condensing temperature (thus pressure) are supplied as input to the heat pump system model in order to get the calculations started; for subsequent iterations, values calculated by the system model are substituted for these estimates.

Heat Exchanger Models

The heat exchanger models, similar to those of Hiller and Glicksman,(5) are predicated on the conventional crossflow configuration and staggered tube and sheet-fin construction. The heat exchanger performance analysis uses equations for the effectiveness as a function of the number of transfer units for a crossflow heat exchanger with both fluids unmixed. The correlations for heat transfer and pressure drop are described in detail in Ref 1, 2, 3, and 5. The air-side heat transfer correlations have been modified for use with wavy rather than smooth fin geometry. The condenser analysis is performed separately for the regions in which the refrigerant is superheated, two-phase, or subcooled. The evaporator analysis is divided into two-phase and superheating regions and accounts for dehumidification of air.

Air-side pressure drops across the heat exchangers and the indoor-air duct system losses were modeled using correlations given by Kirschbaum and Veyo.(6) The indoor-air duct system was assumed to consist of six equivalent parallel ducts with equivalent lengths of 30.5 m (100 ft).

Input parameters for the heat exchanger models include:

- dimensions of the tubing
- geometry of the heat exchangers
- indoor and outdoor dry-bulb temperatures and outdoor relative humidity
- air-flow rates at each heat exchanger
- combined fan and fan-motor efficiency for each heat exchanger

with refrigerant temperature and pressure at entries to the heat exchangers supplied by the system model.

The heat exchanger models calculate:

- heat transfer rates
- refrigerant pressure drops and exit temperatures
- refrigerant subcooling (condenser) or superheat (evaporator) at exit from the heat exchangers
- air-side exit temperatures and pressure drops (including cabinet, filter, and duct losses for the indoor air)
- fan-motor power consumption

Other input parameters to the system model include the dimensions of the interconnecting pipes and the desired values for condenser subcooling and evaporator superheat.

Sequence of Calculations in the Heat Pump Model

The flow chart shown in Fig. 1 outlines the calculational scheme used in this study. After reading the input parameters listed above, the program enters the compressor model which calculates the refrigerant mass-flow rate, power consumed by the motor, and the refrigerant conditions at entry to the condenser. (Initial estimates of condensing and evaporating

temperature are used for the first iteration.) The condenser model in turn produces values for the heat transfer rate, exit air temperature, power consumed by the fan motor, and the refrigerant state at exit from the condenser.

At this point in the calculations, a test is made to see if the subcooling at condenser exit is the desired value. If it is not, the condensing temperature is adjusted and another pass is made through the compressor and condenser models. When the calculated value of subcooling agrees with the desired value, calculations proceed in the evaporator model. The heat transfer rate for this heat exchanger is calculated, along with the changes to refrigerant and air temperatures and pressures, and the fan-motor power consumption.

If the refrigerant superheat at exit from the evaporator is not equal to the specified value, the *temperature of the air* entering the evaporator is adjusted and the evaporator calculation is repeated until the desired superheat is reached. It is not possible to adjust the evaporating temperature at this point, instead of the air temperature, because the refrigerant flow rate, and thus all of the preceeding calculations are dependent on the evaporating temperature that was used in the compressor model.

When the test for desired superheat is satisfied, another test is made, this time to determine if the air temperature entering the evaporator is equal to the specified value. If necessary, the evaporating temperature is adjusted and the calculations for the whole refrigerant cycle are repeated using the values just calculated, rather than the input values for condensing and evaporating temperatures. After all three tests have been satisfied, on condenser subcooling, evaporator superheat, and evaporator entering air temperature, the heat pump capacity and COP can be calculated.

Model Verification

Earlier versions of the heat pump model had been tested against laboratory data to evaluate the accuracy of the calculations.(3) Because the computer programs were modified for this study, it was judged necessary to repeat the validation calculations. The program was executed using the geometric descriptions of a unit in our laboratory, compressor calibration parameters derived from laboratory tests reported by Domingorena,(7) and the operating conditions of run 10 described in that report. The computed performance parameters are in good agreement with observed values from the laboratory test. The calculated mass-flow rates, power consumption, heat exchange rates, and COP fall within 3.5% of the observed values.

Optimization Code and Procedure

The constrained optimization code chosen for this task is a routine prepared by the Numerical Algorithms Group at Harwell, England.(8) The routine is capable of *minimizing* a function subject to equality and/or inequality constraints. To *maximize* the COP subject to the chosen constraints, the function minimized was the negative of the COP plus penalty functions designed to force conformance with the selected constraints.

The procedure used was to specify the desired indoor and outdoor air conditions and initial estimates of the heat pump design parameters, calculate the COP and other performance parameters using the heat pump model, and then let the optimization routine test the results against the constraints. The optimizer then calculated changes in the design parameters to increase the COP while insuring compliance with the constraints. These new design parameters were sent to the heat pump model for the iterative calculation of the COP. The procedure was fully automated on the computer; changes to the design parameters continued until successive improvements to the COP were smaller than the convergence limits of the heat pump model (within one percent).

Optimization Variables

Ten variables were chosen for optimization with regard to steady-state heating efficiency. For *each* heat exchanger, the variables considered are:

- volumetric air-flow rates
- frontal area
- number of tube rows
- number of parallel refrigerant circuits

The two remaining variables are:

- compressor displacement
- refrigerant subcooling at condenser exit

Four of the ten optimization variables, i.e., the number of circuits and tube rows in each heat exchanger, should, of course, be represented by integers. They were treated, however, as being continuously variable; upon completion of the optimization, sensitivity plots were used to determine the most appropriate integer values.

Fixed Geometric Parameters

In order to keep the number of optimization variables to a manageable level, a number of parameters were fixed at values considered typical of present practice. These parameters were judged to have only minor effects on system efficiency. For each heat exchanger, the following parameters were fixed:

- tube spacing in the longitudinal and transverse directions of 25.4 mm (1 in.) and 22.2 mm (0.875 in.), respectively
- inside and outside tube diameters of 8.5 mm (0.33 in.) and 10 mm (0.39 in.), respectively
- fin spacing of 0.55 fins/mm (14 fins/in.)
- fin thickness of 0.16 mm (0.0064 in.)

Interconnecting pipe dimensions were fixed as follows:

- suction line length of 2.4 m (8 ft) and inside diameter of 17 mm (0.68 in.)
- discharge and liquid line lengths of 9.1 m (30 ft) and inside diameters of 14 and 4.8 mm (0.55 and 0.19 in.), respectively

The effective clearance volume ratio of the compressor was fixed at 0.12.

Capacity-Related Constraints

Nominal capacity. For a consistent comparison of various heat pump configurations, the nominal heating capacity was held constant. The nominal capacity value chosen was 11.7 kW (40,000 Btu/h or 3.33 tons) at the ARI high temperature rating point for heating(10). The optimum configuration found for one capacity can, however, be linearly scaled to any other capacity size without affecting the COP(1). Such scaling is facilitated if the capacity-related constraints are appropriately formulated. Therefore the following constraints are discussed as values *per unit of nominal heating capacity:*

- total heat exchanger area
- indoor duct cross-sectional area

Total heat exchanger area. Since the internal geometry of the heat exchangers has been fixed, total heat exchanger area for both coils is directly proportional to the sum of the products of frontal area times the number of tube rows for each coil. This sum, denoted by A_{tot}, will be used to constrain the total available heat exchanger area to physically realizable sizes.* Note that the constraint on the sum of areas is particularly flexible since the optimum ratio of indoor to outdoor coil size can be found while constraining the total available heat exchanger material.

Three values of A_{tot} are considered in the analysis:

- 0.21 m^2/kW (8 ft^2/ton),
- 0.42 m^2/kW (16 ft^2/ton), and
- 0.84 m^2/kW (32 ft^2/ton).

---

*For the chosen internal geometry of the heat exchangers, the total air-side surface area is 22.1 times A_{tot} and the refrigerant-side surface area is 1.06 times A_{tot}.

The value of 0.21 m^2/kW is typical of middle-of-the-line units presently marketed. One top-of-the-line model currently sold has an A_{tot} of 0.36 m^2/kW (13.6 ft^2/ton). Thus the 0.42 and 0.84 m^2/kW cases represent short-term and long-term possibilities, respectively. The larger areas may be considered surrogates for the combined effect of larger and more efficient heat exchangers.

Indoor duct size. Based on the chosen nominal capacity of 11.7 kW (40,000 Btu/h), the diameter of each of the six equivalent circular air ducts was set at 0.2 m (8 in.), i.e., a cross-sectional area of 2.7×10^{-3} m^2/kW (15 $in.^2$/ton). Under this assumption, for an air-flow rate of 0.66 m^3/s (1400 cfm), the duct pressure drop is 0.025 kPa (0.1 in. H_2O) and the combined cabinet and filter pressure drop is 0.075 kPa (0.3 in H_2O). Thus at the indicated flow rate, the indoor air loop of the heat pump system modeled here would have approx. 0.125 kPa (0.5 in. H_2O) total pressure drop when the pressure drop across the indoor coil is included.

Component Efficiency Assumptions

Compressor. Three levels of *maximum* overall compressor efficiency were considered: 48, 56, and 64%. *Actual* overall compressor efficiency can be written as a product of four terms(1,9):

- motor efficiency
- mechanical efficiency
- isentropic efficiency
- suction gas heating efficiency

Maximum overall compressor efficiency is defined here as the product of the first three terms with the motor efficiency given by its maximum rated value. The actual overall efficiency at particular operating conditions differs from the maximum as a result of the changing values of motor efficiency as a function of load and values of suction gas heating efficiency less than 100%. For optimizations at the 8.3°C (47 F) ambient, the motor efficiency was taken to be its maximum value; the calculated suction gas heating efficiencies were between 96 and 98%. The actual overall efficiencies at this ambient are thus 1 to 2 *percentage points* lower than the assumed maximum values. Input parameters for the compressor model that correspond to the chosen compressor efficiencies are shown below.

Maximum overall compressor efficiency (%)	Maximum motor efficiency (%)	Mechanical efficiency (%)	Isentropic efficiency (%)
64	84	95	80
56	84	95	70
48	79	95	64

The particular combinations chosen for a specific maximum overall compressor efficiency may be varied somewhat with minimal effect on the resultant COP and capacity.

Values of overall compressor efficiency for presently manufactured heat pumps range from 42 to 54%. Therefore the 48% case represents an average of present compressor performance. Some current single-speed compressors used in air-conditioners have efficiency values of 56 to 60%. Thus, the 56 and 64% cases represent short-term and long-term compressor performance possibilities, respectively, for heat pump application. The correspondence between the overall compressor efficiency and COP (or EER) for the heat pump and air-conditioning rating conditions as specified in ARI Standard 520-78(11) is as follows:

	ARI 520-78 rating conditions	
Overall compressor efficiency (%)	Heat pump COP (EER)	Air-conditioning EER
64	3.3 (11.2)	10.5
56	2.9 (9.8)	9.2
48	2.5 (8.4)	7.9

Note that for the heat pump rating the COP is calculated on the basis of cooling capacity.

Fans. Two levels of overall fan efficiency (combined fan and fan-motor efficiencies) were selected. Based on the overall efficiencies measured on a heat pump unit tested in our laboratory, base case values of 14% were chosen for the outdoor (evaporator) and 17% for the indoor (condenser) units. For the second level of efficiencies, the base case values were doubled (28 and 34%); such improved efficiencies represent an assumed average between short- and long-term improvement possibilities.

Calculational Procedure

The constraints, fixed parameters, and lists of the parameters that were varied for each computer run are shown in the next section. The nominal heating capacity was maintained at 11.7 kW (40,000 Btu/h) for all calculations referenced to an ambient temperature of 8.3°C (47 F). At this ambient condition, all ten variables were optimized, and the configuration of the optimum design that was consistent with the constraints was fixed in subsequent analysis of the performance at lower ambient temperatures.

Limited optimizations were performed for some of the systems, with an ambient temperature of -8.3°C (17 F), allowing only the refrigerant subcooling at condenser exit and the condenser and evaporator airflow rates to vary. Subsequent analysis of the sensitivity of COP to these design parameters revealed that the values of air-flow rates and subcooling found in the optimization at +8.3°C were suitable also at -8.3°C when

the effects of supplemental resistance heat are considered at lower ambients. Accordingly, the computer runs and results reported here are for system configurations optimized for +8.3°C ambient temperature. The efficiencies reported for -8.3°C outdoor air temperature result from runs of the heat pump model (without the optimizer) using the configuration determined at +8.3°C and allowing the heat pump to assume its "natural" capacity at the lower temperature. Since the compressor motor size was chosen so that the motor would operate at its rated load and speed at ambients of +8.3°C, curves of motor efficiency and speed at part-load conditions were used for the runs at -8.3°C.

The heat pump systems were optimized for various combinations of overall compressor and fan efficiencies and total available heat exchanger area. Results for each system are discussed and compared in the next section.

OPTIMIZATION RESULTS

Calculated Efficiency Limits

Representative results of the optimized heat pump efficiency calculations are shown in Fig. 2 where COPs [at the ARI high temperature rating point for heating(10)] are plotted as functions of available heat exchanger area for three levels of overall compressor efficiency. Selected systems are identified by a system number in parentheses. As reference points, the COPs of our base case (System 1), an optimized "base case" (System 2), and two state of the art (SOA) heat pumps are also shown. The various overall compressor and fan efficiencies are noted on the figure. The values given for overall compressor efficiency are the *actual* instead of the *maximum* values discussed in the previous section and thus include the effects of suction gas superheating inside the compressor shell. The results shown are for 11.7 kW (40,000 Btu/hr) heat pumps; with consistent scaling, the results can be applied to other nominal capacity sizes.

As can be seen from the curves, substantial performance improvement is predicted, compared to today's SOA heat pump. For near-term improvements (System 3) an increase of 28% in steady-state heating efficiency is calculated, for long-range improvements (System 4) a 56% increase is predicted.

Increases in overall compressor efficiency are seen to be uniformly beneficial for all heat exchanger areas considered. For an increase in compressor efficiency of 17% (from 47 to 55%) the COP is improved by 11%. For a 34% increase in efficiency (from 47 to 63%) the performance improvement is 22%.

For a given compressor efficiency, increases in heat exchanger area show eventually diminishing returns. A 100% increase in total available heat exchanger surface shows a 15% increase in performance; a 400% increase in area yields a 29% increase in COP. Thus the last 300% increase in area was required for an improvement equivalent to the first 100%.

The efficiency levels shown by the curves represent the combined result of component improvements and optimized system design. The importance of the optimizing procedure can be seen from its application to the base case heat pump which is typical of today's lower to middle-of-the-line product. As shown in Fig. 2, a 21% improvement in COP (from 2.4 to 2.9) was obtained by optimizing the ten design variables and reducing evaporator superheat (the improvement due to superheat reduction was only 1.7%); no increases in basic component efficiency or heat exchanger area were required. (The 1% increase in overall compressor efficiency was due to a natural reduction in suction gas superheat in the optimized system.) However, the use of more efficient fans with this optimized design improves the COP another 8% for a COP of 3.1 — equivalent to the state-of-the-art, but with smaller heat exchangers and a lower efficiency compressor.

Optimum System Configurations

The system parameters that were fixed for System 1 (base case) and optimized for Systems 2, 3, and 4 of Fig. 2 are compared in Table 1. The COP and heating capacity of these systems are given at 8.3°C (47 F) and at -8.3°C (17 F) ambients. In general, as compared to the base case, the optimized systems require:

- higher air-flow rates
- smaller compressor displacements
- larger frontal areas,
- one-row evaporators
- more parallel refrigerant circuits in the heat exchangers, and
- about 8.3°C (15 F) subcooling at the condenser exit

Sensitivity studies have shown that the COP is fairly insensitive to the number of circuits (above a critical minimum) and to the number of rows of tubes in the condenser (provided the product of rows times frontal area is held constant). The latter insensitivity would allow the use of more condenser rows and proportionally smaller frontal areas to accomodate space limitations of the indoor (condenser) unit. The condenser air-flow rate for the three optimized systems remained approximately the same at values equal to or slightly above the upper limit allowed by ARI for rating purposes.(10) This limit is 60.4 ℓ/s per kW (450 cfm/ton) of nominal capacity, or 708 ℓ/s (1500 cfm) for the nominal capacity chosen for this work.

Optimum Operating Conditions

Table 2 is the counterpart to Table 1 in which calculated operating data are given for the same four systems. Due to the higher condenser air-flow rates in Systems 2, 3, and 4, the indoor-air discharge temperatures are lower. As expected, the R-22 condensing temperatures decrease and the evaporating temperatures increase for the improved systems. The allowable pressure drops are higher in the condenser than in the evaporator, which indicates that for the indoor coil to be used as an evaporator in the cooling mode, the number of circuits should be increased from that found by the optimizer.

Condenser fan power consumption for System 2 is almost twice that for System 1. The increase in indoor air-flow rate results in a substantial reduction in compressor power which more than offsets the increased fan power and thus increases the COP. The optimum indoor air-flow rates remain about the same for Systems 3 and 4, and thus the fan power consumption for these systems is cut in half due to the doubling of the fan efficiency.

Evaporator fan power consumption is significantly smaller for the improved systems due to the large face area of the one-row coils. After the optimizations were completed, an attempt was made to size a fan for these high air-flow rate, low static pressure drop cases. The resulting fan specific speeds were a factor of 2 to 3 higher than currently available with conventional propeller fans. Using 4 to 6 smaller fans in parallel would provide reasonable fan efficiencies; however, the efficiency of small motors is usually low. Costs would be increased significantly.

In this case, the optimum solution for a fixed outdoor fan efficiency resulted in fan requirements which cannot easily be met with currently available fans. However, it is estimated that this difficulty would have more effect on the system configurations than on the resultant COPs. Preliminary calculations suggest that with a 2 or 3-row coil, proportionally smaller frontal areas, and a 25% reduction in outdoor air-flow rates, the fan specific speed could be reduced to achieve the assumed overall fan efficiency of 28% with one or two outdoor fans. Fan power consumption would be on the order of 150 watts. The reduced air-flow rates would result in an increase in the air temperature drop, which in turn would tend to reduce the evaporating temperature. However, the smaller frontal area results in an increase in the face velocity, and thus an increase in the air-side heat transfer coefficient. The net effect is a minimal change in evaporator saturation temperature. In summary, it is estimated that the effect of the reoptimized configuration on the calculated COP would be less than 5% for System 3 and less than 10% for System 4. For future studies, a curve of static efficiency vs specific speed for the outdoor fan will be built into the heat pump model; the optimum configuration will thus be constrained by fan requirements that can be met more easily with currently available fans. For the indoor fan, no such problems were encountered.

Several of the compressor parameters are also given in Table 2. The first two of these, the calculated volumetric efficiency (based on shell inlet conditions) and the mass flow rate of refrigerant, may be used in conjunction with the calculated compressor displacement in the process of compressor selection. For compressors that have equivalent overall compressor efficiency and shell heat loss but differing volumetric efficiencies, the required displacement given in Table 1 can be adjusted(1) to maintain the same refrigerant flow rate. It is important to note that such substitutions can be made without affecting the calculated COP or capacity.

The shell heat loss was calculated for a compressor located in the outdoor unit of a split-system heat pump. The amount of loss could be decreased by indoor siting of the compressor or by arrangements that transfer the heat to the high-side (liquid) refrigerant. Such changes in the shell heat loss would tend to increase the COPs to values higher than those given in Table 1.

The final entries in Table 2 are the required motor shaft power (which is related to motor size) and the compressor-motor power input. A major effect of the improved components and the optimizing procedure is evident in these parameters. In addition to the resultant improvements in COP, the reductions in compressor motor size and compressor displacement partially offset the initial costs incurred by the use of more efficient compressors and larger heat exchangers.

The smaller displacements required by the improved systems might make the use of slower-speed (1725 rpm) compressors again viable for residential application. Although 1725-rpm compressors require twice the displacement of a comparable 3450-rpm compressor, use of the slower-speed compressor in the improved designs would result in compressor displacements only 50 to 70% larger than current 3450-rpm compressors. The slower-speed compressors have the potential for higher overall compressor efficiency, an important consideration in the improvement of heat pump efficiency.

SENSITIVITY OF COP TO CHANGES IN DESIGN PARAMETERS

The optimizing procedure calculates a single set of the "best" design parameters consistent with a given set of constraints; it gives no information about the sensitivity of efficiency to departures from this optimum design. As a practical matter, it is desirable to consider heat pump designs which approximate but may not fully achieve optimum performance. Sensitivity analysis was used to find regions of design flexibility. Such analysis is also useful in determining how the optimum configuration varies with ambient temperature.

General Description of Sensitivity Plots

The sensitivity plots given in this paper show contours of constant values of COP as pairs of design parameters are varied about their optimum values. For each plot the remaining system parameters are held fixed (except for special cases noted later). When appropriate, the plots also contain contours of constant heating capacity which are used to show the effects of the capacity constraint on achievable efficiency levels. The "x" marked on each plot locates the values of the two variables about which the plot was generated. It also denotes, except as noted, the constrained optimum COP.

System 3 of Fig. 2 was chosen as a sample for illustration of the sensitivity analysis.

Sensitivity to Evaporator and Condenser Air-Flow Rates

At 8.3°C (47 F) ambient conditions. Fig. 3 shows the sensitivity of COP to changes in air-flow rates about the optimum configuration for System 3. The "concentric" solid and dashed curves are lines of constant COP and the "diagonal" dashed lines show the combinations of condenser and evaporator air flows that give capacities of 11.7 kW (40,000 Btu/h) and ±2% variations from that value.

In general, the configuration that produces the maximum COP (as a function of air-flow rates) and also provides the required heating capacity will be acheived where the required capacity line is tangent to a line of constant COP.(12) In Fig. 3, this point of tangency occurs at the maximum unconstrained COP value. This particular situation is the best obtainable but it will not be achieved for all possible sets of variables.

The optimum combination of air-flow rates shown in Fig. 3 is the result of tradeoffs between compressor power and fan powers. As the air flows are increased beyond their optimum values, the power consumed by the fans is increased. The compressor power, on the other hand, is reduced because the larger air flows reduce the refrigerant-to-air temperature differences and thus the pressure ratio. However, the increase in fan power dominates, and the net effect is a decrease in COP. Conversely, if the air-flow rates are decreased from the optimum, the compressor power consumption increases faster than fan power decreases; again there is a net decrease in COP.

At -8.3°C (17 F) ambient conditions, no supplemental resistance heat. Fig. 3 was generated for ambient air conditions of +8.3°C (47 F). A similar curve can be generated at lower ambient temperatures to study how the optimum air-flow rates are affected by outdoor air temperatures. Such a plot is shown in Fig. 4 for an ambient temperature of -8.3°C (17 F). No capacity constraint lines are shown on this plot since the heating capacity is allowed to assume its natural value. The optimum COP in Fig. 4 occurs at lower values of air-flow rates than those indicated by the "x". This "x" denotes the optimum values for the +8.3°C (47 F) condition shown in Fig. 3. Fig. 4 indicates that, at lower ambient temperatures, a reduction in air-flow rates is slightly beneficial to the *heat pump* COP. However, since the heating capacity of the heat pump at the -8.3°C (17 F) ambient condition is not sufficient to supply the house demand for the typical application, supplementary resistance heat will be required. Air-flow rates that are more nearly optimum for the combined system (heat pump plus resistance heaters) should instead be considered.

At -8.3°C (17 F) ambient conditions, supplemental resistance heat. In Fig. 5 the effect of resistance heat requirements on the optimum *system* COP is shown. The combined COP was calculated from the equation

$$COP_{sys} = \frac{\dot{Q}_{h(sys)}}{\dot{W}_{sys}} = \frac{1}{\frac{F_{hp}}{COP_{hp}} + (1 - F_{hp})}, \quad (1)$$

where $\dot{Q}_h$ and $\dot{W}$ are heating capacity and input power, the subscripts "sys" and "hp" refer to system and heat pump, and F_{hp} is the fraction of the house load supplied by the heat pump, i.e.,

$$F_{hp} = \frac{\dot{Q}_{h(hp)}}{\dot{Q}_{h(sys)}} . \quad (2)$$

For Fig. 5, $\dot{Q}_{h(sys)}$ was assumed to be 11.7 kW (40,000 Btu/h). Examination of Fig. 5 shows that the optimum system COP of 1.80 (or higher) occurs at condenser and evaporator air-flow rates nearly twice the values found at the +8.3°C (47 F) ambient condition. Thus, the lower air flows found to be optimum for the heat pump at -8.3°C (17 F) in Fig. 4 are farther away from the total system optimum in Fig. 5 than the values chosen for the +8.3°C (47 F) ambient condition. In addition, the extremely high air-flow rates found optimum for the system COP at -8.3°C (17 F) are obviously impractical. Thus the optimum values of air flow for +8.3°C (47 F) ambient condition give reasonably optimum system performance at the -8.3°C (17 F) ambient. For ambient temperatures at and slightly above the system balance point [typically between -2 and 0°C (28 – 32 deg F)] the results of Fig. 4 indicate that a slight reduction in air flows would be beneficial; conversely, above +8.3°C (47 F), a further increase in air flows would be more nearly optimum. However, since conventional multiple-speed fans are more expensive and less efficient, such fine tuning does not appear worthwhile for the heating mode in single-capacity systems.

Sensitivity to Condenser Air-Flow Rate and Ratio of Condenser-to-Total Heat Exchanger Area

The ratio of condenser (indoor) to total heat exchanger area is of interest in regard to both the physical size of the indoor unit and maintenance of low enough evaporator temperatures in the cooling mode for proper dehumidification. The level of evaporating temperature in the cooling mode is also dependent on the indoor air-flow rate. A sensitivity plot of these two parameters in the heating mode can be used to show the design flexibility of the heating COP should air-flow or indoor size compromises be required in the cooling mode.

In order to maintain a constant value for total heat exchanger area, when the indoor-to-total area ratio was changed, the evaporator (outdoor) area was adjusted accordingly. Since the number of tube rows in each coil was held constant, the desired area ratios were achieved by simply adjusting the frontal areas. The outdoor air-flow rate was held constant.

As shown in Fig. 6, the optimum area ratio lies between 0.50 and 0.55. However, with proper adjustment of the condenser air-flow rates, the design capacity (11.7 kW or 40,000 Btu/h) can be maintained over a condenser to total area ratio of 0.37 to 0.67 with a maximum COP loss of 2.5%. The region of interest for proper humidity control in the cooling mode is where the ratios are between 0.37 and 0.55. This is because the smaller indoor-coil surface area and the accompanying lower indoor air-flow rates will result in a lower evaporator temperature in the cooling mode, and thus more moisture removal from the air. For systems with larger total-available heat exchanger area, this ratio becomes an important design question for a reversible heat pump.

Tradeoffs Between Compressor Displacement and Air-Flow Rates

The sensitivity of COP to changes in compressor displacement is not conveniently displayed with contour plots such as those discussed in the preceding paragraphs. Too many parameters must be simultaneously considered because displacement is strongly coupled to both the evaporator and condenser air-flow rates through the capacity constraint.

To examine the effect of variation of the compressor displacement, a series of sensitivity plots similar to that in Fig. 3 was made. Each plot showed the sensitivity of COP to both air-flow rates; a different plot was required for each value of compressor displacement examined. From each plot, the combination of air-flow rates was chosen which gave maximum COP and the desired heating capacity of 11.7 kW (40,000 Btu/h).

Fig. 7 shows the results of this analysis for System 3. COP and the associated optimum air-flow rates are plotted against compressor displacement. Note that the higher values of compressor displacement require lower air-flow rates to achieve maximum COP that is consistent with the capacity constraint. The curve of COP vs displacement shows that variations of ±10% in displacement are possible with only a 2% loss in COP provided that air-flow rates are properly adjusted. The evaporator air-flow rates for the lower values of displacement do, however, become quite high.

In Fig. 8, a series of COP vs displacement curves are shown starting with the base case point and moving sequentially to Systems 2 and 3 with intermediate systems also included. Each curve was generated in the same way as Fig. 7. The successive curves show the cumulative effect of one additional type of system improvement on the width of the COP "plateau"

and on the optimum values of COP and displacement. Note that as the systems are improved, the widths of the plateaus become narrower. This implies that there is less flexibility in the improved designs and that good design techniques become more critical. However, in all the systems considered, there is some design flexibility with regard to the "optimum" displacements and associated air-flow rates.

There would be more flexibility if the sensitivity analysis were extended to include the ratio of indoor-coil area to total heat exchanger area. The curves in Fig. 8 could be further broadened by conducting three-variable optimizations (subject to the capacity constraint) over the range of displacement values. The variables in this case would be the two air-flow rates and the area ratio. If the displacement were allowed to vary far from the original optimum, the other variables (condenser subcooling and number of circuits and rows) should also be re-optimized.

SUMMARY AND CONCLUSIONS

The study reported in this paper focused on the development of a design method — one that takes advantage of optimization techniques to maximize the COP obtainable with component efficiencies and heat exchanger size limitations specified by the designer. To illustrate its use, the method was applied with particular sets of assumptions about component efficiencies for a range of heat exchanger sizes. Flexibility in the choice of design parameters was explored by sensitivity analysis. The rather qualitative conclusions drawn from this work follow:

1. The optimizing design method is an efficient means of maximizing system efficiency.

The calculated heating mode efficiencies show the possibility of significant improvement in steady-state heating efficiency. Application of the method to the base case heat pump showed that significant improvement (20%) is possible without changing any component efficiencies or increasing heat exchanger area. Thus the increase in COP for the other cases presented is attributable in part to the improved components, but also to the optimization of the system configuration. The short-term improvement case with higher component efficiencies and larger heat exchangers showed a 28% increase in COP over the best commercially available heat pumps (65% compared to our base case). The long-term case showed a 56% increase over state of the art (83% over the base case). The technique also allows the designer to compare the relative efficiency benefits due to a variety of component improvements while holding the nominal heating capacity constant. It thereby provides a rational basis for deciding where to make the best investments in improved efficiency.

2. Sensitivity analysis is needed to take best advantage of design flexibilities.

The optimization procedure searches for a "best" system configuration. The sensitivity analyses indicate that there is not a single best configuration,

but rather a family of designs with near-optimum performance and constant heating capacity. Tradeoffs between parameters are possible (in the vicinity of an optimum) that allow flexibility in the choice of components without significant loss in COP.

Tradeoffs between compressor displacement and air-flow rates were shown to allow a range of operating conditions with near-maximum COP for various compressor displacement choices. The sensitivity analyses also show that the range of flexibility is significantly narrower for the higher efficiency systems; the need for careful application of design techniques is evident.

3. The initial application of the optimizing design technique indicates that more work would be useful.

Results of system optimizations must be carefully examined to insure that reasonable bounds of current technology are not exceeded. An example is the difficulty we experienced in trying to size propeller fans for the specific speed and static efficiency implied by the calculated outdoor air-flow rates and pressure drops. Future versions of the model should include equations to circumvent this problem.

In this study, the design method was applied to optimize the heating efficiency of a conventional heat pump. However, application of the method is not limited to the heating mode; it can be applied to cooling-mode performance with constraints to ensure good humidity control. These results, combined with heating-mode optimizations, would form a more complete specification of a high-efficiency conventional heat pump. Furthermore, the generality built into the models makes them applicable to unconventional heat pumps as well. The use of an optimizing technique and a physically-based heat pump model in the design of variable-speed heat pumps (which are inherently more complex) would be particularly appropriate.

REFERENCES

1. C. K. Rice, et al., *Design Optimization and the Limits of Steady-State Heating Efficiency for Conventional Single-Speed Air-Source Heat Pumps*, (to be published).

2. R. D. Ellison and F. A. Creswick, *A Computer Simulation of Steady-State Performance of Air-to-Air Heat Pumps*, ORNL/CON-16 (March 1978).

3. R. D. Ellison et al., "Heat Pump Modeling: A Progress Report," *Proceedings of the Fourth Annual Heat Pump Technology Conference*, Oklahoma State University, Stillwater, Oklahoma, April 9–10, 1979.

4. J. K. Martin and D. L. O'Neal, *An Energy and Cost Analysis of Residential Heat Pumps*, ORNL/CON-49 (to be published).

5. C. C. Hiller and L. R. Glicksman, *Improving Heat Pump Performance via Compressor Capacity Control-Analysis and Test,* Report No. 24525-96, Heat Transfer Laboratory, Massachusetts Institute of Technology (1976).

6. H. S. Kirschbaum and S. E. Veyo, *An Investigation of Methods to Improve Heat Pump Performance and Reliability in a Northern Climate,* Vol. III, pp. B1–8, Electric Power Research Institute, EPRI EM-319 (January 1977).

7. A. A. Domingorena, *Performance Evaluation of a Low-First-Cost, Three-Ton, Air-to-Air Heat Pump in the Heating Mode,* ORNL/CON-18 (October 1978).

8. Numerical Algorithms Group, *NAG Fortran Library. Mark 7,* Atomic Energy Establishment, Harwell, England (1978).

9. R. W. Shaffer and W. D. Lee, "Energy Consumption in Hermetic Refrigerator Compressors," *Proceedings of the 1976 Purdue Compressor Technology Conference,* Ray W. Herrick Laboratories, West Layfayette, Indiana July 6–9, 1976.

10. Air-Conditioning and Refrigeration Institute, *Standard for Air-Source Unit Heat Pump Equipment,* ARI-240-77 (1977).

11. Air Conditioning and Refrigeration Institute, *Standard for Positive Displacement Refrigerant Compressors, Compressor Units and Condensing Units,* ARI 520-78 (1978).

12. W. F. Stoecker, *Design of Thermal Systems,* McGraw-Hill, Inc., New York, NY, pp. 126–27 (1971).

Table 1. Performance and Configuration of the Base Case and Three Optimized Systems

	System #			
	1	2	3	4
Performance				
At 8.3°C (47 F) ambient				
COP	2.40	2.92	3.96	4.90
Heating capacity, kW (MBtu/h)	11.8 (40.4)	11.7 (40.1)	11.7 (40.0)	11.7 (39.9)
At -8.3°C (17°F) ambient				
COP	2.11	2.36	3.13	3.55
Heating capacity, kW (MBtu/h)	7.71 (26.3)	7.44 (25.4)	7.32 (25.0)	6.97 (23.8)
Constraints				
Maximum overall compressor efficiency, %	48	48	56	64
Overall fan efficiency, %				
Indoor	17	17	34	34
Outdoor	14	14	28	28
Relative heat exchanger area	1	1	2	4

Table 1. continued

	System #			
	1	2	3	4
Design Parameters				
Condenser (indoor coil)				
Air-flow rate, ℓ/s (cfm)	566 (1200)	732 (1550)	708 (1500)	755 (1600)
Frontal area, m^2 (ft^2)	0.31 (3.35)	0.41 (4.40)	0.65 (6.94)	1.42 (15.3)
Number of tube rows	3	3	4	4
Number of circuits	3	2	4	6
Subcooling, °C (F)	28 (50)[a] 17 (30)[b]	8.9 (16)	7.2 (13)	9.4 (17)
Evaporator (outdoor coil)				
Air-flow rate,				
Air-flow rate, ℓ/s (cfm)	1090 (2300)	1580 (3350)	2270 (4800)	3300 (7000)
Frontal area, m^2 (ft^2)	0.51 (5.50)	1.25 (13.5)	2.25 (24.2)	4.21 (45.3)
Number of tube rows	3	1	1	1
Number of circuits	4	6	7	8
Superheat, °C (F)	11 (19)[a] 1.7 (3.0)[b]	1.7 (3.0)	1.7 (3.0)	1.7 (3.0)
Compressor				
Displacement, mℓ ($in.^3$)	68.9 (4.20)	58.4 (3.56)	56.3 (3.43)	50.8 (3.10)

[a]value at 8.3°C (47 F) ambient condition

[b]value at -8.3°C (17 F) ambient condition

Table 2. Operating Conditions of the Base Case and Three Optimized Systems at 8.3°C (47 F) Outdoor Temperature

	System #			
	1	2	3	4
Condenser (indoor coil)				
Air discharge temp., °C (F)	38.4 (101.2)	34.4 (94.0)	34.8 (94.7)	33.9 (93.1)
R-22 exit sat. temp., °C (F)	54.4 (130.1)	40.2 (104.3)	37.5 (99.5)	35.5 (95.9)
R-22 pressure drop, kPa (psi)	14.5 (2.1)	217 (18.4)	48.2 (7.0)	53.7 (7.8)
Fan power, W	343	640	265	290
Evaporator (outdoor coil)				
R-22 exit sat. temp., °C (F)	-3.39 (25.9)	-2.39 (27.7)	0.11 (32.2)	2.55 (36.6)
R-22 pressure drop, kPa (psi)	49.6 (7.2)	16.5 (2.4)	20.7 (3.0)	24.1 (3.5)
Fan power, W	375	106	52	50
Compressor				
Volumetric efficiency, % (based on shell inlet conditions)	64.3	76.5	80.1	82.8
R-22 mass flow rate, g/s (lbm/h)	45.8 (363)	49.9 (396)	54.3 (431)	54.9 (435)
Shell heat loss, W (Btu/h)	946 (3230)	735 (2510)	478 (1630)	366 (1250)
Motor shaft power, W (hp)	3350 (4.49)	2580 (3.46)	2230 (2.99)	1720 (2.30)
Compressor-motor input power, W	4210	3270	2650	2040

ORNL–DWG 79-10736

THE ORNL HEAT PUMP MODEL CALCULATES ENERGY BALANCES FOR THE PRINCIPAL COMPONENTS OF THE HEAT PUMP

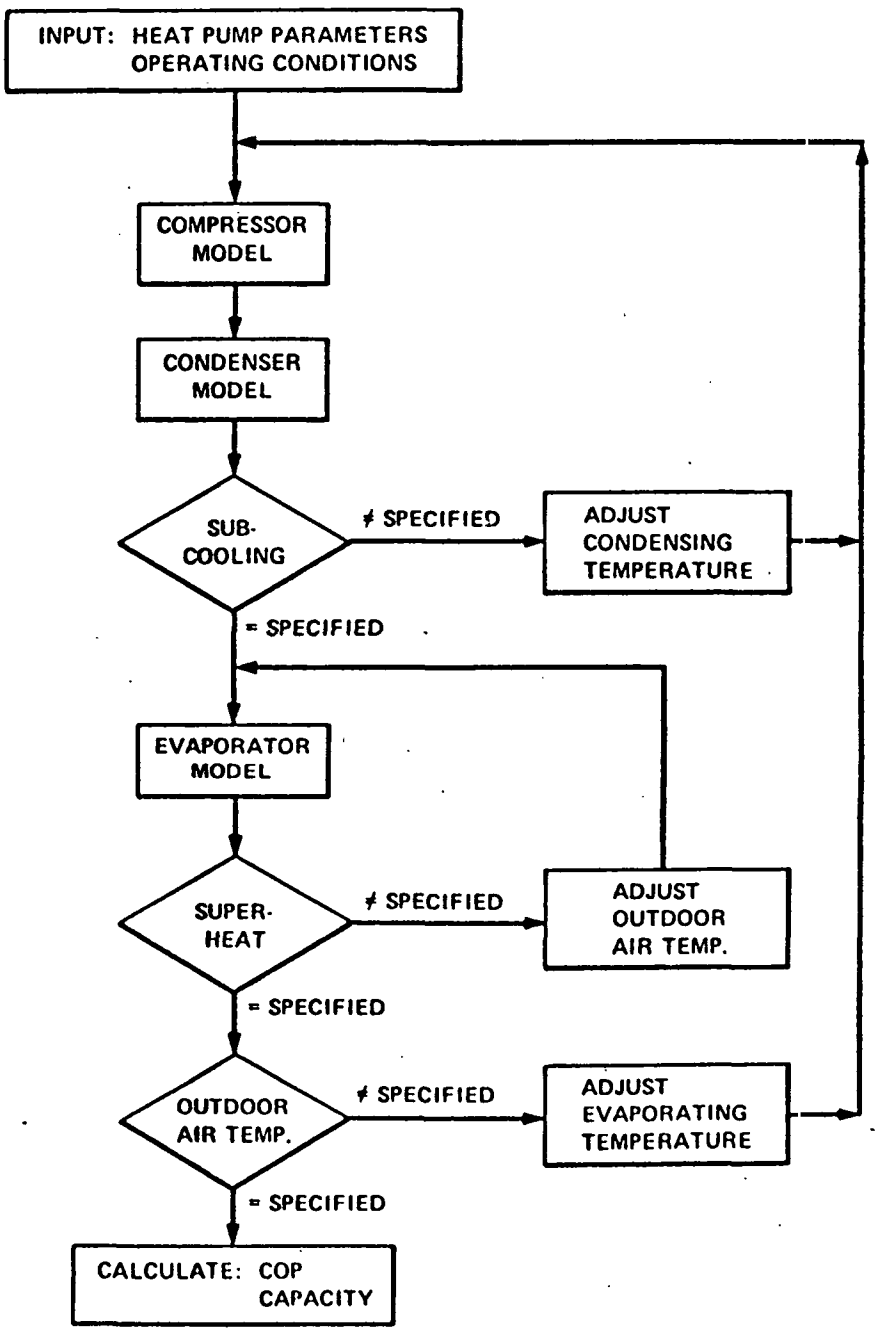

Fig. 1. Flow diagram of the heat pump model used for design optimization

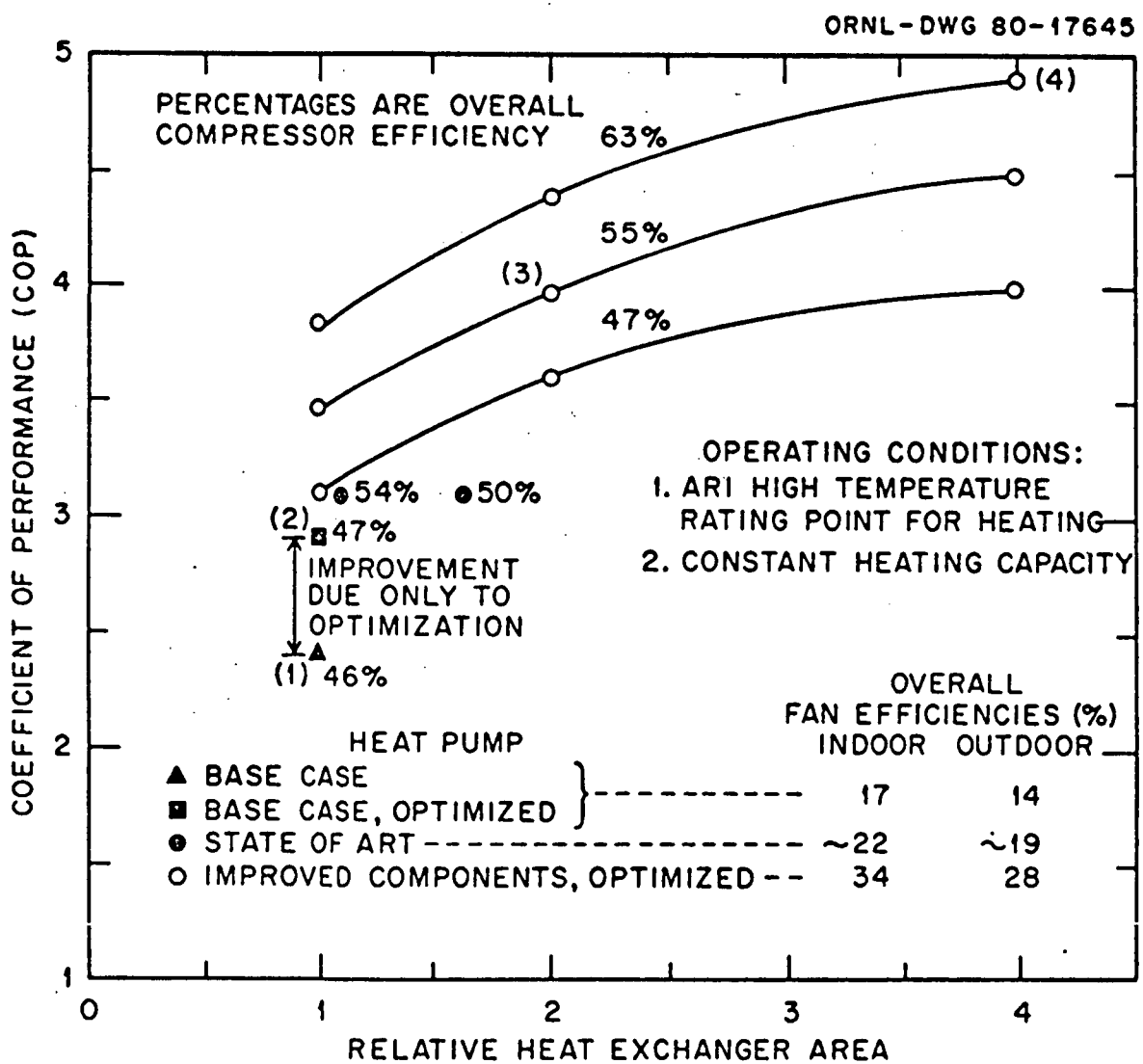

Fig. 2. Effects of compressor efficiency, heat exchanger area, and design optimization on heat pump COP

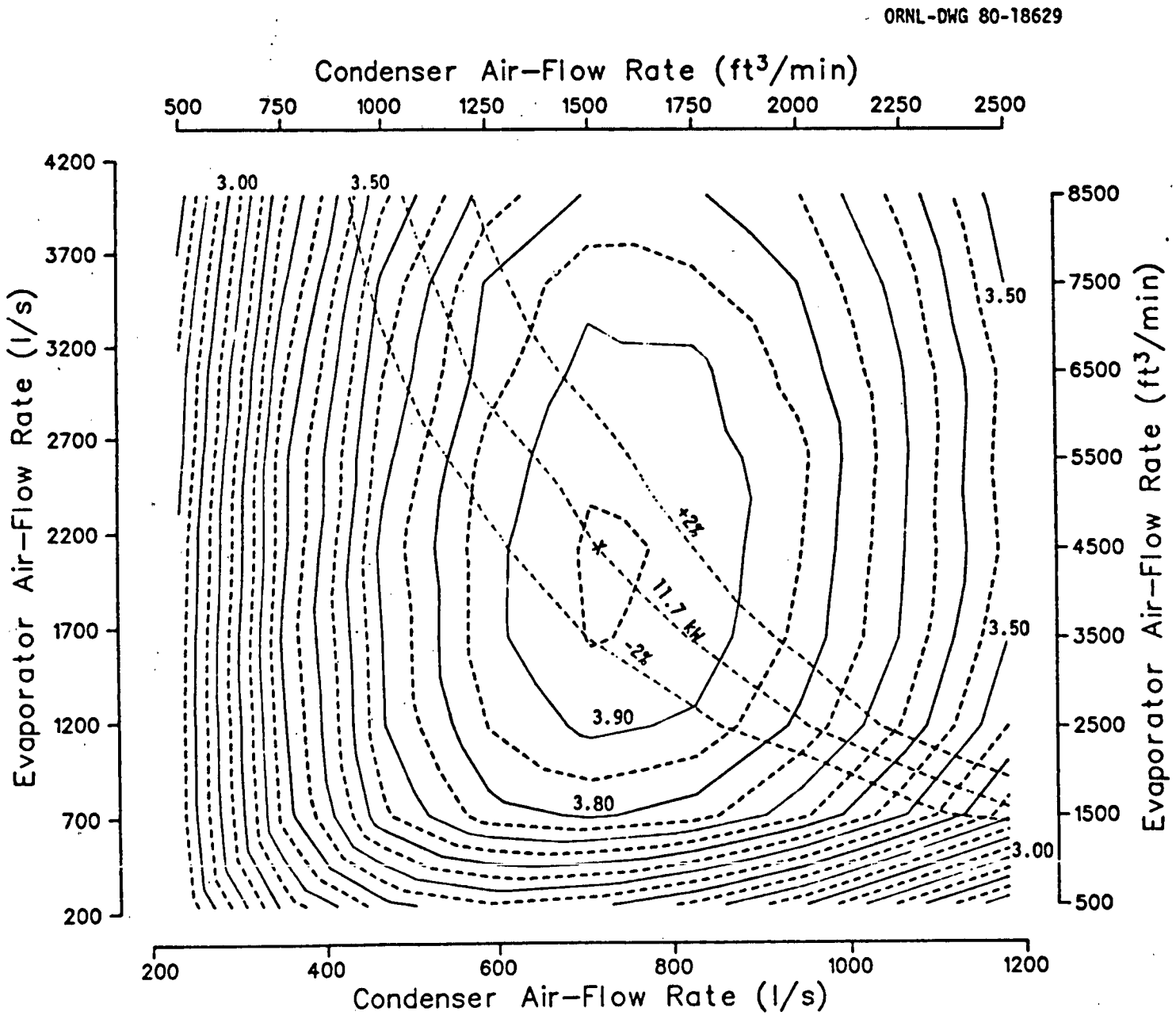

Fig. 3. Sensitivity of COP and heating capacity to air-flow rates at 8.3°C (47 F) outdoor temperature - System 3

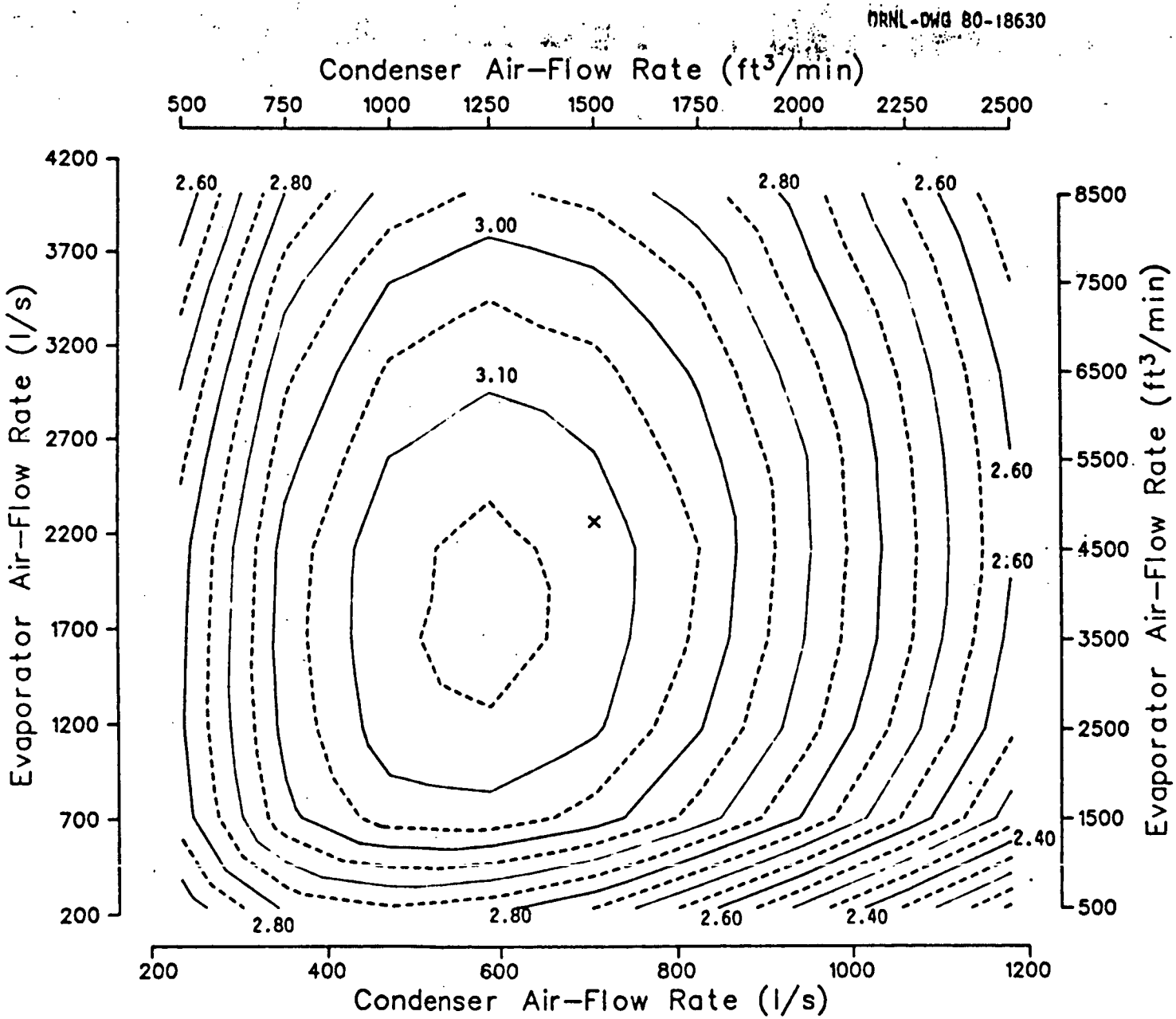

Fig. 4 Sensitivity of COP (with no supplemental resistance heat) to air-flow rates at -8.3°C (17 F) outdoor temperature - System 3

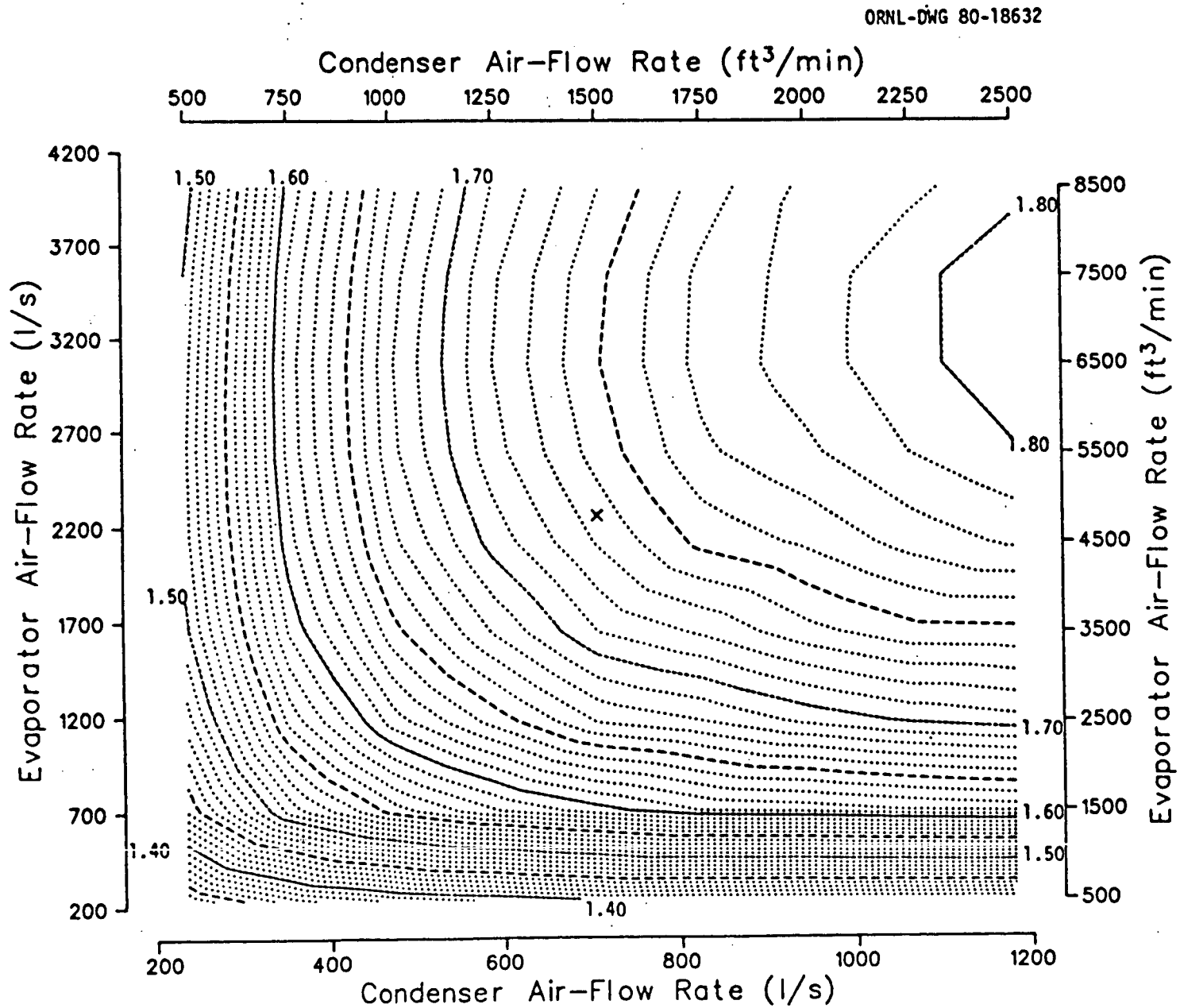

Fig. 5 Sensitivity of COP (with supplemental resistance heat) to air-flow rates at -8.3°C (17 F) outdoor temperature - System 3

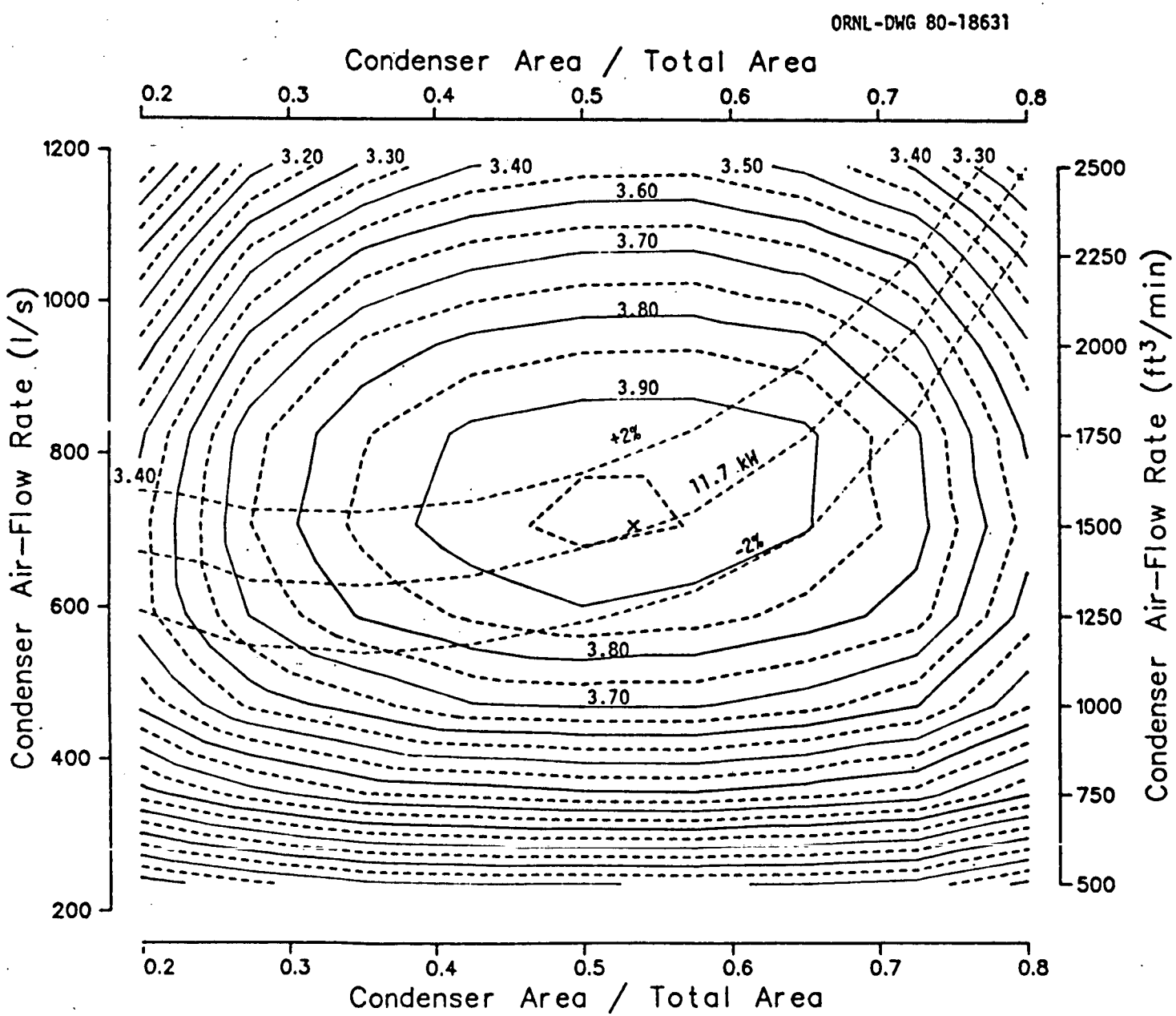

Fig. 6 Sensitivity of COP and heating capacity to condenser air-flow rate and area ratio at 8.3°C (47 F) outdoor temperature - System 3

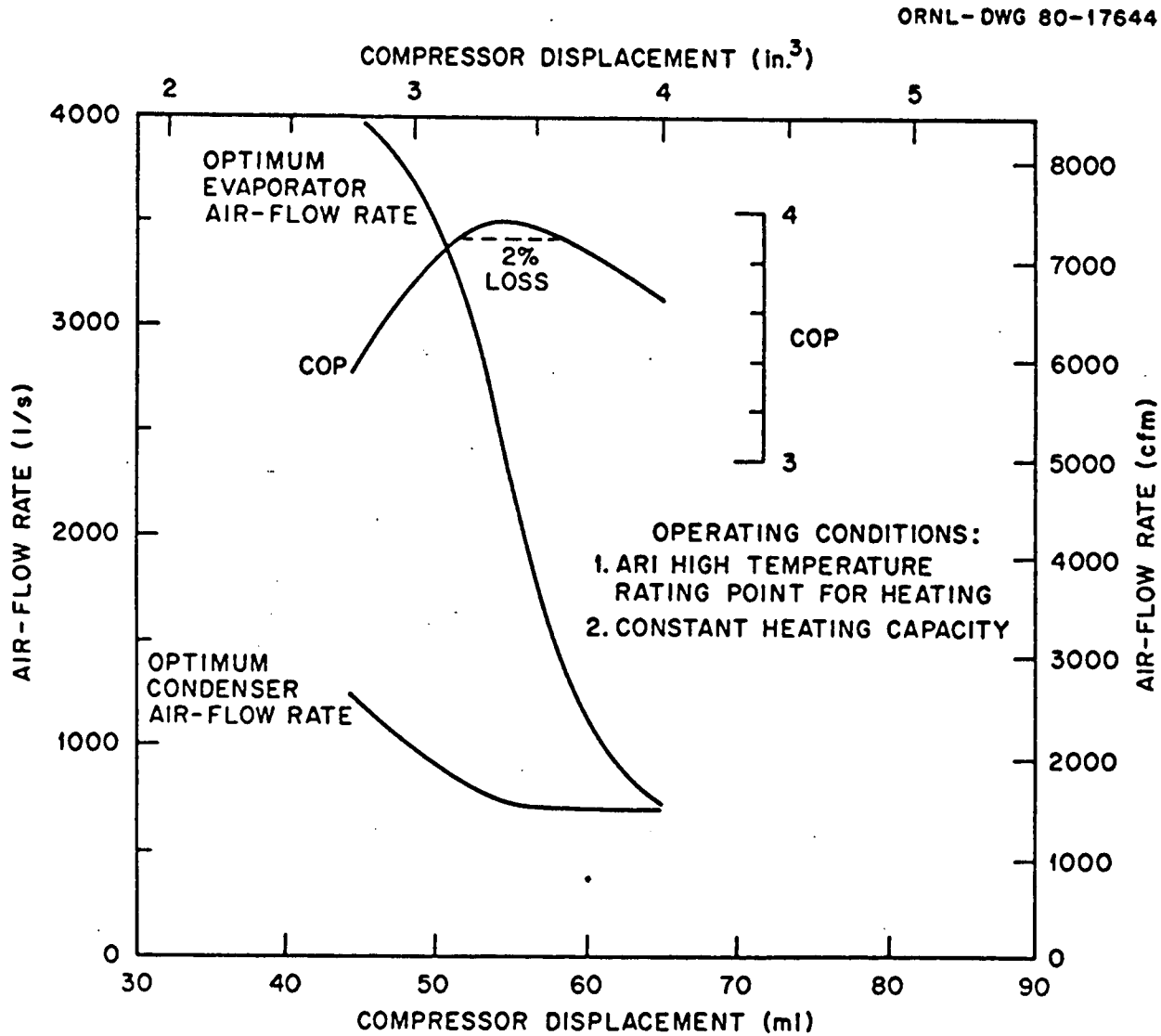

Fig. 7 COP and air-flow rates vs compressor displacement for System 3

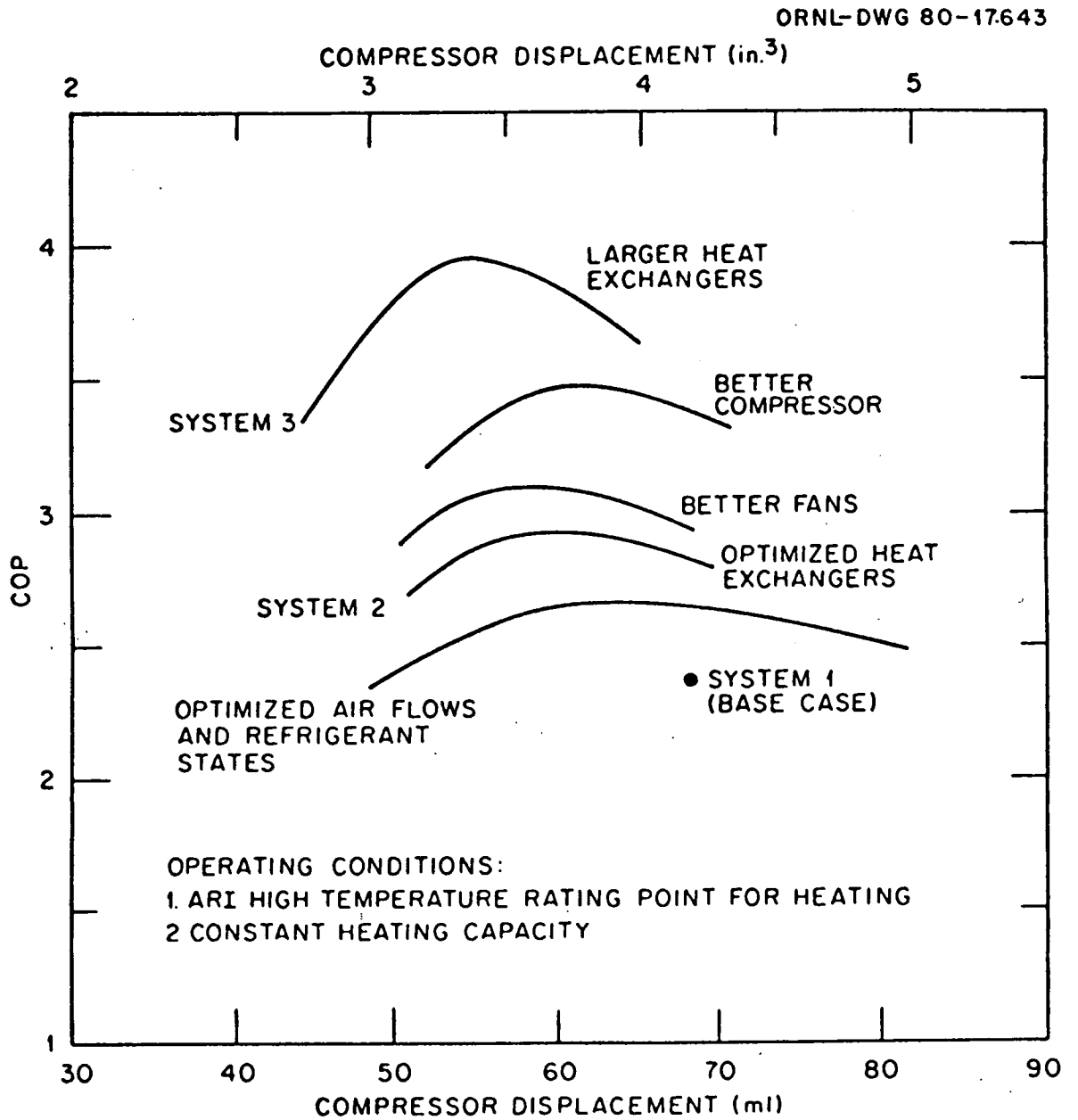

Fig. 8 COP vs compressor displacement for a series of successive improvements from the base case system